BioNanoScience (2018) 8:769–777
https://doi.org/10.1007/s12668-018-0538-z

Quantitative Cytotoxicity, Cellular Uptake and Radioprotection Effect of Cerium Oxide Nanoparticles in MRC-5 Normal Cells and MCF-7 Cancerous Cells

Nouraddin Abdi Goushbolagh[1] · Bagher Farhood[2] · Akram Astani[3,4] · Abolfazl Nikfarjam[5,6] · Mojgan Kalantari[7] · Mohammad Hosein Zare[5,6]

Published online: 18 June 2018

Abstract

Optimal distribution of cerium oxide nanoparticles (CONPs) or nanoceria can have a significant impact on their cytotoxicity, cellular uptake, and radioprotection effects. In this study, two different distribution plans of CONPs were investigated. A scanner electron microscope (SEM) was used for chemical analysis and recording of CONP images. Using MTT assay, the non-toxic concentrations of nanoceria with two different distribution plans were determined in MRC-5 and MCF-7 cell lines. Nanoceria cellular uptake at 50, 150, and 250 μM with two different dispersion plans was determined by using the U*V*/VIS absorbance of cell culture medium after 24 h of incubation. In order to quantify radioprotection effect, cells treated with non-toxic concentrations of nanoceria were exposed to 10, 40, and 100 cGy of 6 MV photon beams. The diameter of the spherical CONPs was 29 nm. Energy dispersive spectroscopy analysis showed that the cerium element has the highest weight percentage in CONPs (97.9%). Accumulation rate of filtered and non-filtered suspension were determined as 0.3608 and 14.2708 μg/ml/h, respectively. The 70 and 110 μM concentration of sustained nanoceria suspension did not have any toxicity for MRC-5 and MCF-7 cells, respectively. In both cell lines, 50, 150, and 250 μM of filtered nanoceria had a significant uptake than the non-filtered nanoceria. A total of results showed that the 70 μM of nanoceria have a significant radioprotection on normal cells in the radiation dose of 40 and 100 cGy, while the highest cellular uptake of nanoceria occurred in cancer cells. The results suggest that using of stable distribution of CONPs for radiation protection could be a good choice, knowing that these nanostructures will have selective protection in normal cells.

Keywords Cerium oxide nanoparticles · Radioprotection effect · MTT assay · MRC-5 · MCF-7

✉ Mohammad Hosein Zare
mhzare2009@gmail.com

1 Department of Medical Physics, Faculty of Medicine, Shahid Sadoughi University of Medical Sciences, Yazd, Iran

2 Department of Medical Physics and Radiology, Faculty of Paramedical Sciences, Kashan University of Medical Sciences, Kashan, Iran

3 Zoonotic Diseases Research Center, School of Public Health, Sahid Sadoughi University of Medical Sciences, Yazd, Iran

4 Department of Microbiology, Faculty of Medical Sciences, Shahid Sadoughi University of Medical Sciences, Yazd, Iran

5 Department of Medical Physics, Faculty of Medicine, Shahid Sadoughi University of Medical Sciences, Yazd, Iran

6 Radiotherapy Research Center, Shahid Sadoughi University of Medical Sciences, Yazd, Iran

7 Department of Radiology, Mahdiyeh Hospital, Shahid Beheshti University of Medical Sciences, Tehran, Iran

1 Introduction

Ionizing radiation is a dangerous and unwanted factor for work health in space travels, nuclear plants, and medical imaging; as an example, ionizing radiation exposure with high dose can cause destructive effect on normal tissues that are mostly observed in cancerous patients who have been cured with ionizing radiation [1–3]. Transported energy from a photon or a particle to atom or molecule as a result of a direct modification means a chemical conversion of macromolecule that can be important for a biological activity. Vital events inside the nucleus and DNA structure can induce damage and double-strand break. These inner events lead to two mechanisms: one is direct DNA damage by radiation energy and the other is indirect effect of radiation energy by particles of radical intermediates, peroxide and superoxide, which are produced by radiolysis of water [4, 5]. Therefore, for work irradiation and incidence of secondary cancer after treatment by

radiotherapy, protecting healthy tissue is becoming increasingly important by using appropriate shielding or modern devices that have been optimized in order to the reduce radiation exposure for patient and radiation workers. Furthermore, a remarkable process in radiotherapy is the use of radiosensitizers and radioprotectors as free radical damage moderators [4, 6–8]. Biologically, cerium oxide nanoparticles (CONPs) or nanoceria act as a catalyst, like the antioxidant enzyme superoxide dismutase, and due to its large surface to volume ratio have an individual electrical structure so that they cause oxygen reduction. Active places on the surface of CONPs can act as a free radical scavenger. Recently, these nanostructures are being checked as interventional treatments in biological systems. The scavenging of free radicals by nanoparticle performance is the inhibition of reactive oxygen species (ROS). These species are highly unstable and reactive, as they capture cellular macromolecule electrons that results to their inefficiencies [9–12].

Designing the smart multipurpose nanostructures for intracellular imaging and target therapy requires a complete understanding conduction mechanism of nanoparticles into cells. For clinical and biological applications, the ability to control and inhibit nanoparticle accumulation in cells for a long time can lead to improvement in diagnostic sensitivity and treatment efficiency. So, scrutinization of nanoparticles' performance in cell will result in better understanding of nanoparticle uptake and cytotoxicity [13]. It is quite obvious the slight differences in physicochemical nanoparticles will lead to significant biological consequence in cellular uptake and biological processes of nanoparticles [14, 15].

Ultimately, using CONPs for controlling the free radicals induced by radiation can be a qualified procedure for inhibition of radiation damage. These nanoparticles have a long half-life in comparison with other radiation protection compounds such as amifustin, because of their self-regeneration properties. According to the 2007 recommendations of the International Commission on Radiological Protection (ICRP), the lung tissue weight factor is equal to 0.12. Nevertheless, the value for the liver, thyroid gland, and skin is 0.05, 0.05, and 0.01, respectively. It means that human fibroblast lung cells (MRC-5 cells) are the most sensitive to ionizing radiation and it will be the most damaged in comparison with other tissues under the same conditions of irradiation [6, 16, 17]. Furthermore, optimal distribution of CONPs can have a significant impact on their cytotoxicity, cellular uptake, and radioprotection effects.

Therefore, in the current study, the cytotoxicity of nanoceria and cellular uptake in two different distribution plans (filtered and non-filtered) was determined. To this end, MRC-5 and cancerous epithelial breast cell line, MCF-7, was chosen. Finally, the stable suspension of nanoceria was used in the radiobiology study; as to the best of our knowledge, the current research is the first study on evaluating the radioprotection effect of CONPs in MRC-5 cell lines.

2 Materials and Methods

2.1 Characterization of Cerium Oxide Nanoparticles

CONPs (cerium oxide nanopowder, CeO2, 99.97%, 10–30 nm) from US research nanoparticles were purchased. A scanning electron microscope (SEM, Phenom, Phenom Prox) and transmission electron microscope (TEM, ZEISS, LEO 906) with 100 KeV were used to characterize the shape and dimension of CONPs. The chemical composition of CONPs was determined using energy-dispersive spectroscopy (EDS, Phenom, Phenom Prox) in region mode with a resolution of Mn $K\alpha \leq 140$ eV. Cerium oxide nanopowder was dissolved in distilled water; also it was sonicated for 15 min to prevent agglomeration of nanoparticles. Finally, nanoceria suspensions were propagated on a carbon grid and electron microscopic images were recorded. All the measurements were carried out at room temperature (25 °C). The absorption spectra of CONPs in 300 μg/ml concentration were recorded by a spectrophotometer (U*V*/VIS Double Beam Spectrometer), and the maximum absorption wavelength was determined. The absorbance of suspensions was prepared at concentrations of 1, 100, 200, and 300 μM at maximum wavelength (λ_{max}), and the standard curve was plotted (XLABEL: Concentration, YLABEL: Absorbance).

2.2 Preparation of Nanoceria Suspension

The suspension of nanoceria was sterilized by 70% ethyl alcohol. Sterile stocks of suspensions were mixed up with vortex for 2 to 3 min, and finally, they were sonicated at room temperature for 2 h by ultrasound sonication (D-78224 Singen/Htw). In order to prepare a filtered suspension, after sonication, they were passed through a 0.22-μm filter and their concentration was determined from the standard curve immediately. At the same time, the concentration of unfiltered CONPs was also determined. Both suspensions were conserved for 24 h and their U*V*/VIS absorption was recorded by a spectrophotometer and their secondary concentration was determined. At the end, the accumulation rate of both suspensions was calculated and compared with each other.

2.3 Cell Staining

In this stage, the cells were first fixed with 10% formalin and then stained with crystal violet solution. Finally, the plate was washed with water and cell images were observed using a microscope (Zeiss), and images were captured at × 10 magnification (Sony, Cyber-shot, DSCWX200 camera).

2.4 Cell Culture

The MRC-5 and MCF-7 cell lines were prepared from the Iranian biological research center and were cultured in DMEM/F12 and DMEM High Glucose medium containing 10% fetal bovine serum plus penicillin antibiotics (100 IU/ml) and streptomycin (100 μg/ml) in T25 flasks, respectively, and kept in an incubator in condition of 5% CO_2 at 37 °C.

2.5 Cytotoxicity and MTT Assay

For designation of toxicity effect and the rate of growth and proliferation of cells treated with CONPs after the irradiation process, the MTT assay (3- [4,5-dimethylthiazol-2-yl]-2,5-difenyl-tetrazolium bromide) was used. This is a mitochondrial competition metabolic test and based on the breakdown of tetrazolium salt by the mitochondrial enzyme succinate dehydrogenase in living cells [18]. In this test, the cells with 20,000 cells/well density were cultured in each 96-well microplate wells. 0, 0.5, 1, 2, 3, 4, 5, 6, 7, and 8 μM concentrations of non-filtered CONPs and 0, 5, 10, 30, 50, 70, 110, 150, 200, 250, and 300 μM of filtered CONPs were added to wells containing MRC-5 and MCF-7 cells. After 3 h, the medium of wells was replaced and incubated for 24 h. Eventually, the MTT color was added to the wells at a concentration of 20 mg/ml (5 mg/ml dissolved in PBS) and was incubated at 37 °C for 3 h. The cells were then washed with PBS buffer, and 150 μl of DMSO (Cinagen®, Iran) was added to each well and placed on a shaker for 10 min. In the next step, optical density (OD) of wells was read by an ELISA reader (the Biotech Instrument Model: Box998) at a reference wavelength of 570 nm (triplicate).

2.6 Cellular Uptake

To check CONP cellular uptake, 2×10^5 cells for each cell lines were cultured in 96-well plates. Twenty-four hours after incubation, the cells were treated with three concentrations of 50, 150, and 250 μM of nanoceria suspensions in two distribution plans (filtered and non-filtered) as previously mentioned. After 3 h, the medium of cells was replaced and incubated at 5% CO_2 and 37 °C for 24 h. The cells were separated from the wells by trypsin and reached to 3 ml volume. Then, they were mixed up by vortex to allow the cells to be completely lysed and the absorbed nanoparticles were released by the cells. Ultimately, the absorbance of U*V*/VIS radiation for 36 microtubes was determined by a spectrophotometer and the concentration of each suspension was determined by the corresponding standard chart.

2.7 Radioprotection Effect

The cells treated in the non-toxic concentrations of CONPs were exposed to doses of 0 (control group), 10, 40, and 100 cGy. The mean cell survival percentage of the irradiated groups was determined by MTT assay after 24 h of incubation. The cells were irradiated with 6-MV X-rays emitted from Siemens Oncor (Siemens Healthcare, Erlangen, Germany) at the dose rate of 300 cGy/min in Ramezanzadeh Radiotherapy Center (Yazd, Iran).

2.8 Statistical Analysis

The quantitative variables were analyzed using Excel software. Then, *P* values were calculated using one-way ANOVA and Tukey tests for comparing different groups. The 95% confidence level was considered as the statistical significance level of the results.

3 Results and Discussion

3.1 Characterization of Cerium Oxide Nanoparticles

The nanoparticle morphology and size are one of the important factors in their biological behavior. The SEM photograph indicates some agglomeration and aggregation. Furthermore the diameter of these nanoparticles was determined as 29.3 nm (Fig. 1a). It can be seen from the high-resolution TEM analysis that nanoceria crystals have a polygon structure with 25–50-nm sizes (Fig. 1b). It is notable that according to application of nanoparticles, their sizes can be achieved by various methods of synthesis and preparation of nanoparticle suspensions to the desired dimensions [19].

Based on Fig. 1c, the histogram plotted by EDS analysis for CONPs, 73,015 particles were counted in 3 s that is marked by a red curve (recorded by detector) with three peaks. Moreover, according to the white curve (simulated by software), oxygen peak was observed only in 0 to 1 KeV voltage range. In the rest of the voltage range, only the cerium element was counted. As for EDS analysis, two elements of cerium and oxygen were distinguished in 97.9 wt.% (with a confidence level of 97.5%) and 2.1 wt.% (with a confidence level of 81.5%), respectively (Table 1).

The U*V*/VIS absorption spectrum of CONPs dissolved in deionized water was plotted as shown in Fig. 2a. The maximum absorption occurred at 318 nm with an absorption value of 0.5041. Therefore, in subsequent readings, for the plotting of standard curve and also in specifying the absorption of CONPs by cells, the wavelength of 318 nm was used for readings. The absorbance of CONP suspensions was recorded at concentrations of 1, 100, 200, and 300 μM at a wavelength of 318 nm, and the standard curve of CONPs was plotted as shown in Fig. 2b. In some studies, the CONPs have the highest absorption at wavelengths of 310 and 298 nm. The reasons for these differences can be as follows: (1) different

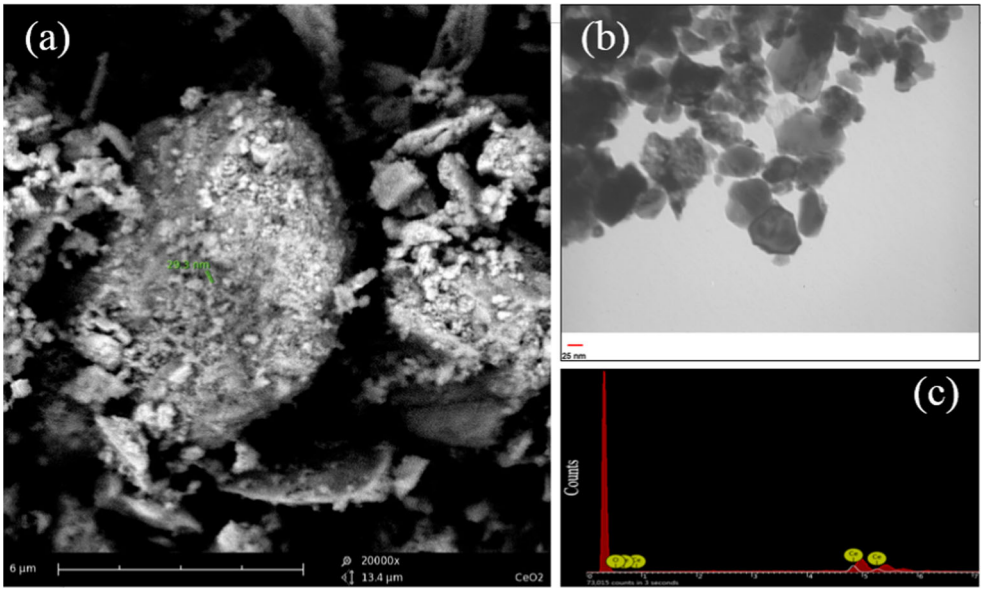

Fig. 1 **a** SEM images. **b** TEM images of CONPs. **c** Energy-dispersive spectroscopy analysis of CONPs in region mode

models of spectrophotometer, (2) differences in the quality of the cuvette, (3) different calibration of devices, (4) different syntheses of CONPs, and (5) different diameters of nanoparticles [20–22].

The mean absorbance (at 318 nm) of CONP suspensions with an initial concentration of 3000 μg/ml after filtering was 0.0857. The absorbance of the suspension after 24 h was 0.0840. Non-filtered nanoceria suspension with initial concentration of 430 μg/ml was prepared, and after 24 h, the UV/VIS adsorption rate was 0.0170. The initial and secondary concentrations (after 24 h) were assigned by the standard curve of Fig. 3b for both filtered and non-filtered suspensions, where the accumulation rate of suspensions was calculated as follows:

$$\text{Accumulation rate of filtered suspension} = \frac{431-422.5\ (\mu g/ml)}{24\ (h)} = 0.3608\ {}^{\mu g}/_{ml.h}$$

$$\text{Accumulation rate of non-filtered suspension} = \frac{430-87.5\ (\mu g/ml)}{24\ (h)} = 14.2708\ {}^{\mu g}/_{ml.h}$$

Table 1 The chemical analysis of energy-dispersive spectroscopy in the region mode to assess the constituent elements and their weighting percentage in cerium oxide nanoparticles (CONPs). The cerium element with atomic number 58 has the highest percentage weight in CONPs

Element name (element symbol)	Atomic number	Concentration (%)	Certainty (%)	Error (%)
Cerium (Ce)	58	97.9	97.5	2.5
Oxygen (O)	16	2.1	81.5	18.5

With regard to the calculated accumulation rate for both filtered and non-filtered suspensions, clearly, in the non-filtered state, CONPs do not have a stable distribution.

3.2 Cytotoxicity Measurements

The penetration of nanoparticles into cell membranes is an interesting phenomenon that may have important outcomes for biomedical applications of nanoparticles. Cellular uptake

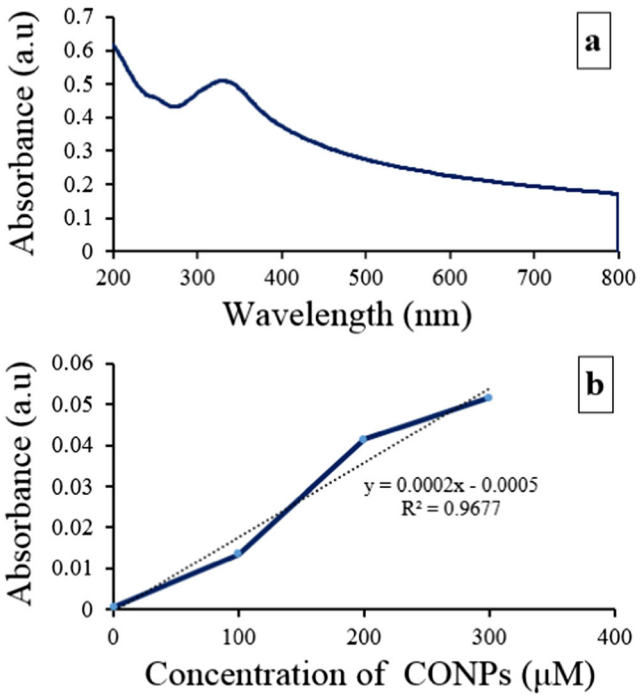

Fig. 2 **a** The UV/VIS absorption spectrum of cerium oxide nanoparticles (CONPs) using a double-beam atomic absorption spectrophotometer. **b** Standard curve of CONPs

and cytotoxicity of CONPs are two factors that are influenced by the distribution of CONPs.

Owing to the results of MTT assay for the determination of IC_{10} (concentration of nanoparticles, which leads to 10% cell inhibition), the filtered suspension of CONPs was more toxic in comparison with the non-filtered suspension in the both cell lines, which may be due to the homogeneous distribution of nanoparticles in the deionized aqueous medium. In the non-filtered distribution plan, CONPs had a lower cytotoxicity compared to the other distribution plan in both cell lines because the results showed less cellular uptake for this plan. Therefore, the distribution of nanoparticles can play a significant role in determining their toxicity [23].

Figure 3 shows the natural morphology for MRC-5 and MCF-7 cell lines. According to the screenshots, normal lung fibroblastic cells (MRC-5) have spindle-shaped and cord-like structures. On the other hand, breast cancer cells (MCF-7) were spherical approximately. According to Fig. 3, the size of the MRC-5 cells is four times larger than that of the MCF-7 cells approximately. Based on practical experience, normal cells had a slower growth rate than cancer cells.

The toxicity of CONP suspension was defined in filtered and non-filtered states for MRC-5 and MCF-7 cell lines (Fig. 4). According to the results of the MTT test in Fig. 5, non-filtered CONP suspensions in MRC-5 and MCF-7 cell lines did not demonstrate any toxicity up to concentrations of 4 and 7 μM. Furthermore, the filtered CONP suspension demonstrated higher toxicity than non-filtered CONP suspension, so that the non-toxic concentration for MRC-5 and MCF-7 cell lines was determined as 70 and 110 μM, respectively.

The non-toxic concentration of CONPs was designated to be 70 μM (24.08 μg/ml). In various studies, concentrations of 2.5 and 3.5 μg/ml were determined as IC_{10} of nanoceria.

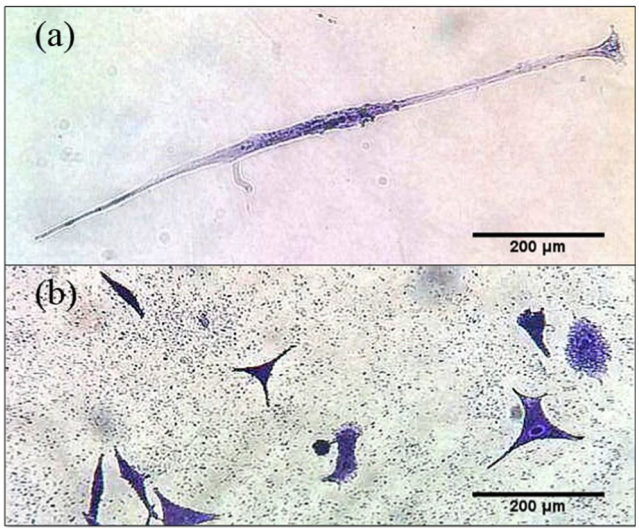

Fig. 3 Morphology of cell lines stained with crystal violet. (**a**) MRC-5 normal cell lines. (**b**) MCF-7 cancerous cell lines

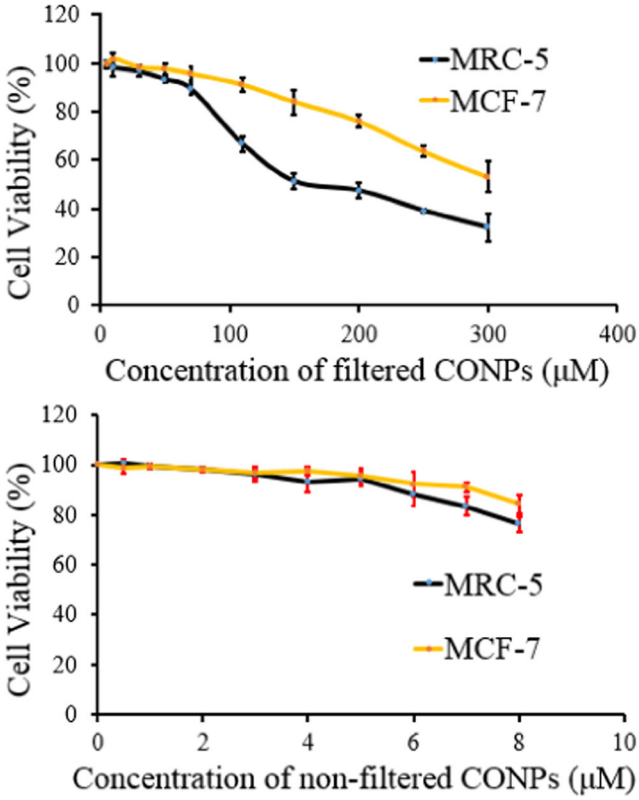

Fig. 4 MRC-5 and MCF-7 cells viability for determination of cytotoxicity was measured by MTT assay. The cell treated with filtered nanoceria suspension (**a**) and non-filtered nanoceria suspension (**b**). Percent of toxicity = (ODtest/ODcontrol) × 100. Experiment was performed three times

According to the results of the studies, nanoparticle distribution and size, cell line, and cell viability assay can affect the cytotoxicity determination of the CONPs [24–28].

3.3 Determination of Cellular Uptake

As shown in Fig. 5, the highest cellular uptake in MRC-5 cells was specified for 150-μM filtered CONPs, which was 81.71 ± 32.67. On the other hand, for MCF-7 cells, the highest cellular uptake of CONPs occurred at the concentration of 250 μM, which was 170.93 ± 20.50 μM. Given the results presented in Fig. 5, the amount of CONP absorption in both cell lines significantly increased with increment of stability in the distribution of CONPs. In the survey of normal cells, the *P* values for the significant increment of the mean cell viability of treatment groups with 50, 150, and 250 μM concentrations of filtered CONPs than non-filtrated CONPs at same concentrations were 0.45, 0.00, and 0.00, respectively. In the same conditions, the *P* values of 0.37, 0.00, and 0.00 were obtained for cancer cells. Also, cellular uptake of CONPs in MCF-7 cell line was higher than that in MRC-5 cell line (at same concentrations of CONPs). The difference in cellular uptake can be due to the high rate of proliferation of cancer cells relative to normal cells.

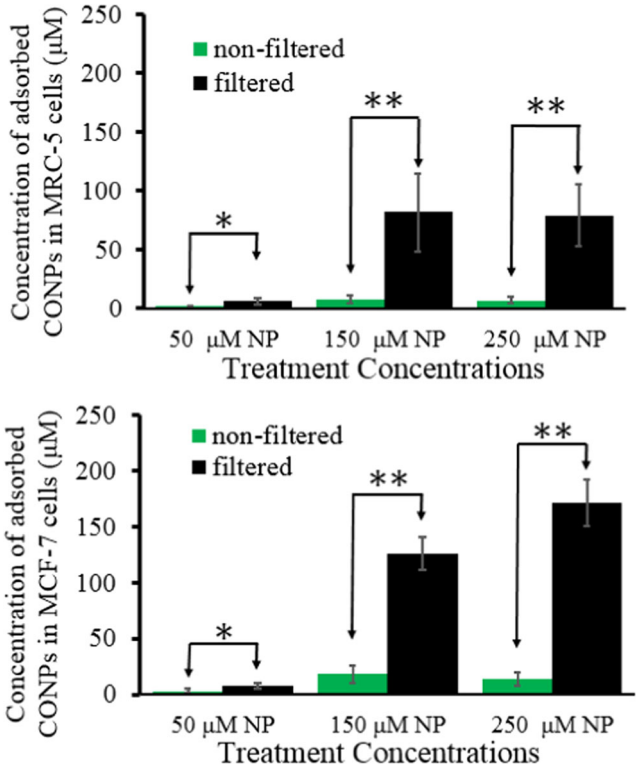

Fig. 5 Investigation of cerium oxide nanoparticle absorption with different (filtered and unfiltered) distributions in MRC-5 and MCF-7 cell lines. Groups were labeled with * showed a significant increase in cellular absorption than the control group (non-filtered nanoceria suspension) at similar concentrations, with a P value < 0.05. Also, the groups were labeled with a ** have a P value < 0.001

The process of cellular uptake, like cytotoxicity, is affected by some parameters such as size, morphology, superficial charges, and distribution of CONPs. Cellular uptake of non-filtered nanoceria decreased in both MRC-5 and MCF-7 cell lines with increasing of concentrations from 150 to 250 μM, but this decreasing was not significant (P-values were 0.838 and 0.660, respectively). However, slight decrease and no increase in cellular uptake with increment of non-filtered CONPs concentration indicates that increment of CONPs concentration can lead to increased accumulation. Therefore, the desirable cellular uptake will not occur because of the instability in the distribution [29–32].

The toxicity of solvent or metal nanoparticles in micron sizes depends on the solubility of the elements in the solvent or on the chemical stability of the particles. One of these metal nanoparticles that can reduce biological conductivity is CONPs consisting of Ce (3+) and Ce (4+) [29, 33]. The results of the cellular uptake in this study suggest that by filtration of the CONPs, the particles are separated in dimensions of 0.20 μm and their superficial charge leads to the removal of nanostructures, resulting in the attraction factor not able to lead to the accumulation of nanoparticles. Hence, the stable distribution of nanoparticles will result in favorable cellular uptake. By filtration, an optimal distribution of CONPs can be achieved, while the use of surfactants for optimization of CONP distribution can lead to more toxicity.

3.4 Radioprotection Effects of Cerium Oxide Nanoparticles

Given that the main purpose was to protect healthy cells, so, the dose of CONPs (filtered suspension) was used that had no toxicity for MRC-5 cells. The cells were treated with 5, 10, 30, 50, and 70 μM of CONPs. As shown in Fig. 6, the mean cell viability (%) of MRC-5 cells exposed to the radiation dose of 10 cGy increases with increment of CONP concentration, but it was not significant (P value > 0.05). Also, the results of one-

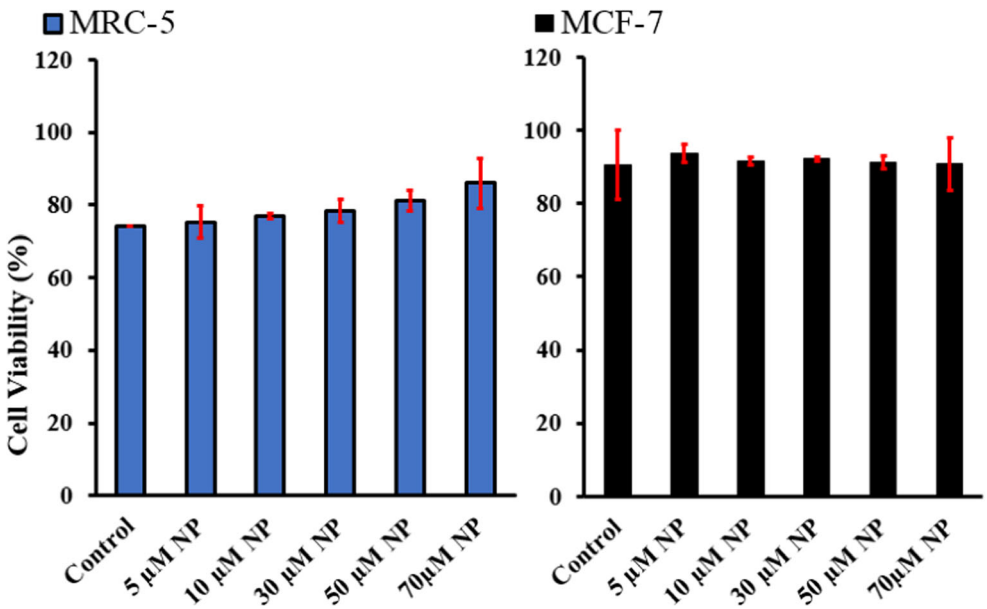

Fig. 6 MRC-5 and MCF-7 cell viability for determination of radioprotection effect was measured by MTT assay. The cells were irradiated with 6-MV X-rays at the 10-cGy radiation dose in the presence of cerium oxide nanoparticles

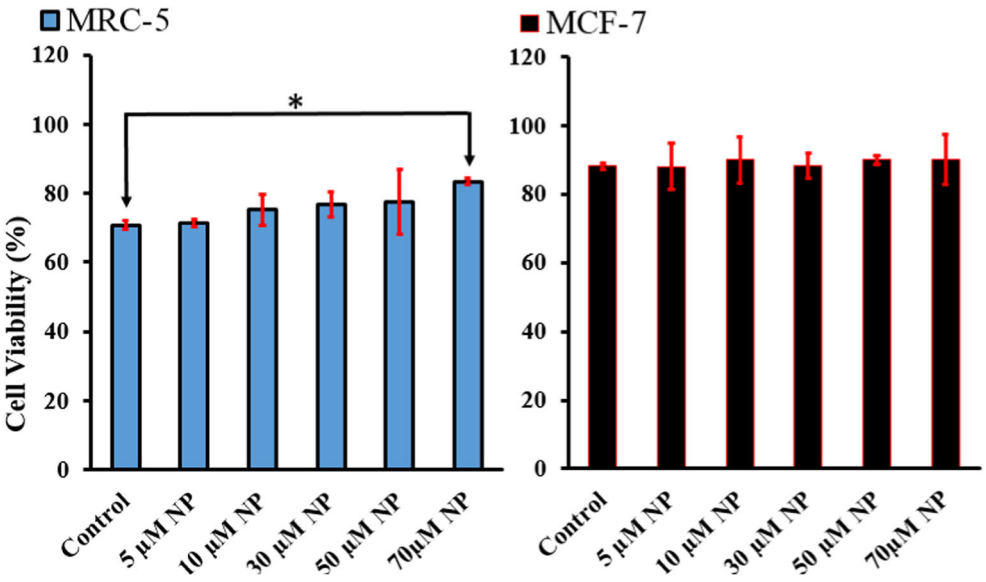

Fig. 7 MRC-5 and MCF-7 cell viability for determination of radioprotection effect was measured by MTT assay. The cells were irradiated with 6-MV X-rays at the 40-cGy radiation dose in the presence of cerium oxide nanoparticles. Data, expressed as percentage of cell viability, are means ± SD of six experiments for each cell lines. The groups labeled with * have a P value < 0.05

way ANOVA indicated that there was no overall significant increase between treated groups and control group in mean cell viability (%) for cancer cells (P value > 0.05).

The finding (Fig. 7) showed the changes of mean cell viability (%) at the 40 cGy radiation dose are not significant with increasing CONP concentration for cancerous cells. Nevertheless, the mean cell viability (%) at 70 μM for normal cells (83.49 ± 0.85) was significantly higher than for the control group (70.81 ± 1.16) (P value = 0.049).

As seen from Fig. 8, in 100 cGy radiation dose, treated groups in the normal cells with a concentration of 70 μM compared to 0, 5, 10, and 30 μM had a significant increase in the mean cell viability (P values were 0.001, 0.002, 0.003, and 0.012, respectively). In addition, substantial radiation protection was observed in the presence of 50 μM CONPs compared to those of 0, 5, and 10 μM (P values were 0.013, 0.025, and 0.037, respectively). Furthermore, the changing of mean viability of cancerous cells (%) was not significant in the presence of CONPs at 100 cGy radiation dose (P value > 0.05). The use of CONPs to reduce the oxidative stress of cigarette smoke showed that cell death rates have been reduced by the presence of nanoceria in the H9C2 cell lines that has been treated with cigarette smoke, compared to those who did not receive nanoceria; so that in the CONP concentrations of 1, 10, and 100 nM, the cell death dropped 10, 30, and 20%, respectively compared to the cells that did not receive CONPs [12]. In the other study, the effect of CONP radiation protection in normal lung cells (CCL 135) at a concentration of 10 nM (0.0017 mg/ml) were investigated in both cases before and after exposure to 20 Gy radiation dose. In both cases, a

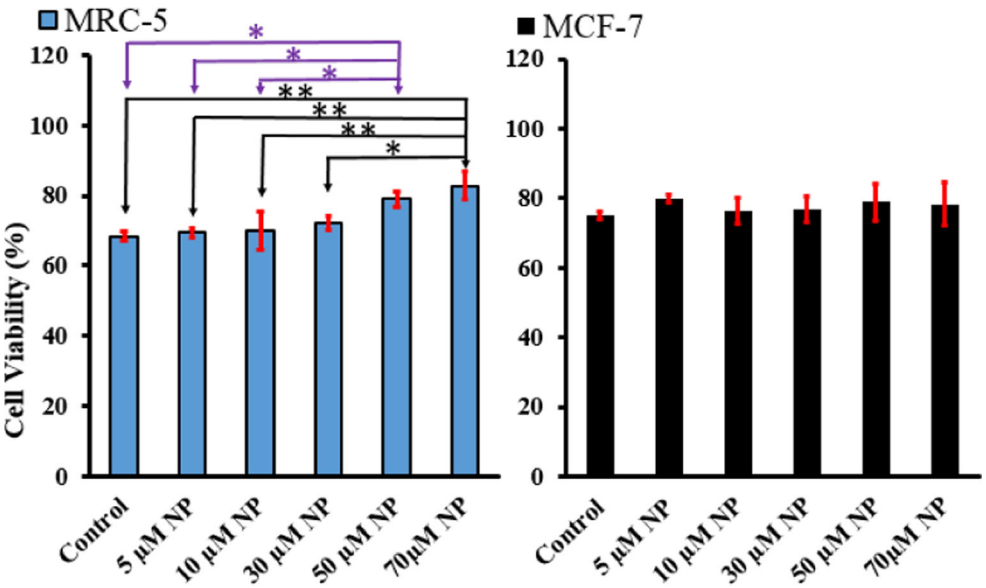

Fig. 8 MRC-5 and MCF-7 cell viability for determination of radioprotection effect was measured by MTT assay. The cells were irradiated with 6-MV X-rays at the 100-cGy radiation dose in the presence of cerium oxide nanoparticles. Data, expressed as percentage of cell viability, are means ± SD of six experiments for each cell lines. The groups labeled with * and ** have P < 0.01 and P < 0.001, respectively

significant protective effect was observed by CONPs [34]. Ultimately, the use of CONPs as well as similar-function compounds can reduce the probability of deterministic and stochastic damages after exposure of ionization radiation. Applying CONPs in cancer radiotherapy can allow the oncologist to prescribe an optimal irradiation dose with higher safety margin to eliminate tumor tissue.

Extensive studies have been conducted to investigate the radiation protection effects of CONPs, but the most desirable results will be achieved when the best radiation protection is obtained from the lowest concentration of CONPs. As shown in Fig. 8, increasing the concentration of CONPs from 50 to 70 μM does not result in significant radiation protection in normal cells per 100 cGy irradiated dose. Therefore, using a concentration of 70 μM cannot be justified, because 50 μM concentration of CONPs can result in significant radiation protection compared to the control group. Increasing the cellular uptake of nanoceria will lead to an increase in the scavenging of free radicals caused by radiation. However, because of the increased growth rate of cancer cells versus normal cells after 24 h, the ratio of nanoparticles absorbed to the number of cells will decrease in the cancer cells and, as a result, the process of the free radicals scavenging will be slowing down which can be a reason for the lack of significant radiation protection in cancer cells while this ratio will be steady or slower reduction in normal cells.

According to statistical analysis results, completely different changes in the mean cell viability (%) were observed for the two cell lines of MRC-5 and MCF-7, so that increment of mean cell viability (%) in normal cells, due to an increase of CONPs concentration, was significant at 40 and 100 cGy radiation doses. However, the presence of CONPs in cancer cells have not caused significant radiation protection which indicates the effect of the selective radiation protection of CONPs [34].

It is noteworthy that quantifying cytotoxicity and cellular uptake of CONPs with consideration of other parameters such as incubation time and use of surfactants as nanoparticle distribution stabilizers, can clarify the pathway to more accurate and better studies for perusing the role of CONP radiation protection.

4 Conclusion

CONPs play an important role in scavenging free radicals and can be introduced as a powerful radioprotector against ionizing radiation. The elimination of confounding factors, such as the accumulation of nanoceria, as well as the determination of optimal non-toxic concentrations with respect to sensitive cell lines, is important in this type of studies. According to the results, the cell line and the CONP distribution can be effective in determining the cytotoxicity and cellular uptake of CONPs. The filtered CONPs had higher uptake rates than non-filtered CONPs, and this rate was higher in cancer cells due to the high rate of cell proliferation. Furthermore, CONPs at higher radiation doses can provide significant protection against ionizing radiation in normal cells (MRC-5), but this radiation protection will not occur in cancerous cells (MCF-7). However, the presence of nanoceria in normal tissue cannot be a reason for the lack of precision in the treatment planning.

Acknowledgements This article was extracted from a master's thesis in medical physics by the first author and it was supported by Shahid Sadoughi University of Medical Sciences, Yazd, Iran. We most especially acknowledge the friendly cooperation of the Shahid Remezanzadeh radiation oncology workers in Yazd, Iran.

Compliance with Ethical Standards

Conflict of Interest The authors declare that they have no conflict of interest.

References

1. Najafi, M., Motevaseli, E., Shirazi, A., Geraily, G., Rezaeyan, A., Norouzi, F., et al. (2018). Mechanisms of inflammatory responses to radiation and normal tissues toxicity: Clinical implications. *International Journal of Radiation Biology, 94*, 335–356.
2. Yahyapour, R., Motevaseli, E., Rezaeyan, A., Abdollahi, H., Farhood, B., Cheki, M., et al. (2018). Reduction-oxidation (redox) system in radiation-induced normal tissue injury: molecular mechanisms and implications in radiation therapeutics. *Clinical and Translational Oncology* (in press).
3. Yahyapour, R., Motevaseli, E., Rezaeyan, A., Abdollahi, H., Farhood, B., Cheki, M., et al. (2018). Mechanisms of radiation bystander and non-targeted effects: Implications to radiation carcinogenesis and radiotherapy. *Current Radiopharmaceuticals, 11*, 34–45.
4. Wang, C., Blough, E., Dai, X., Olajide, O., Driscoll, H., Leidy, J. W., et al. (2016). Protective effects of cerium oxide nanoparticles on MC3T3-E1 osteoblastic cells exposed to X-ray irradiation. *Cellular Physiology and Biochemistry, 38*, 1510–1519.
5. Alavi, S. S., Dabbagh, S. T., Abbasi, M., & Mehrdad, R. (2017). Medical radiation workers' knowledge, attitude, and practice to protect themselves against ionizing radiation in Tehran Province, Iran. *Journal of Education and Health Promotion, 6*, 58–64.
6. Velpula, N., Ugrappa, S., & Kodangal, S. (2017). A role of radioprotective agents in cancer therapeutics: a review. *International Journal of Basic & Clinical Pharmacology, 2*, 677–682.
7. Jafarpour, S. M., Safaei, M., Mohseni, M., Salimian, M., Aliasgharzadeh, A., & Fahood, B. (2018). The radioprotective effects of curcumin and trehalose against genetic damage caused by I-131. *Indian Journal of Nuclear Medicine, 33*, 99–104.
8. Safaei, M., Jafarpour, S. M., Mohseni, M., Salimian, M., Akbari, H., Karami, F., et al. (2018). Vitamins E and C prevent DNA double-strand breaks in peripheral lymphocytes exposed to radiations from iodine-131. *Indian Journal of Nuclear Medicine, 33*, 20–24.
9. Hirst, S. M., Karakoti, A. S., Tyler, R. D., Sriranganathan, N., Seal, S., & Reilly, C. M. (2009). Anti-inflammatory properties of cerium oxide nanoparticles. *Small, 5*, 2848–2856.

10. Nelson, B. C., Johnson, M. E., Walker, M. L., Riley, K. R., & Sims, C. M. (2016). Antioxidant cerium oxide nanoparticles in biology and medicine. *Antioxidants, 5*, 15–35.
11. Vávrová, J., Řezáčová, M., & Pejchal, J. (2012). Fullerene nanoparticles and their anti-oxidative effects: a comparison to other radioprotective agents. *Journal of Applied Biomedicine, 10*, 1–8.
12. Niu, J., Wang, K., & Kolattukudy, P. E. (2011). Cerium oxide nanoparticles inhibits oxidative stress and nuclear factor-κB activation in H9c2 cardiomyocytes exposed to cigarette smoke extract. *The Journal of Pharmacology and Experimental Therapeutics, 338*, 53–61.
13. Chithrani, B. D., & Chan, W. C. (2007). Elucidating the mechanism of cellular uptake and removal of protein-coated gold nanoparticles of different sizes and shapes. *Nano Letters, 7*, 1542–1550.
14. Alwan, A., MacLean, D. R., Riley, L. M., d'Espaignet, E. T., Mathers, C. D., Stevens, G. A., et al. (2010). Monitoring and surveillance of chronic non-communicable diseases: Progress and capacity in high-burden countries. *Lancet, 376*, 1861–1868.
15. Petri-Fink, A., Steitz, B., Finka, A., Salaklang, J., & Hofmann, H. (2008). Effect of cell media on polymer coated superparamagnetic iron oxide nanoparticles (SPIONs): colloidal stability, cytotoxicity, and cellular uptake studies. *European Journal of Pharmaceutics and Biopharmaceutics, 68*, 129–137.
16. Baker, C. H. (2013). Harnessing cerium oxide nanoparticles to protect normal tissue from radiation damage. *Translational Cancer Research, 2*, 343–358.
17. Valentin, J. (2007). *The 2007 recommendations of the international commission on radiological protection*. Oxford: Elsevier.
18. Mosmann, T. (1983). Rapid colorimetric assay for cellular growth and survival: Application to proliferation and cytotoxicity assays. *Journal of Immunological Methods, 65*, 55–63.
19. Lee, C. L., Wan, C. C., & Wang, Y. Y. (2001). Synthesis of metal nanoparticles via self-regulated reduction by an alcohol surfactant. *Advanced Functional Materials, 11*, 344–347.
20. Sujana, M., Chattopadyay, K., & Anand, S. (2008). Characterization and optical properties of nano-ceria synthesized by surfactant-mediated precipitation technique in mixed solvent system. *Applied Surface Science, 254*, 7405–7409.
21. Karakoti, A. S., Singh, S., Kumar, A., Malinska, M., Kuchibhatla, S. V., Wozniak, K., et al. (2009). PEGylated nanoceria as radical scavenger with tunable redox chemistry. *Journal of the American Chemical Society, 131*, 14144–14145.
22. Zhang, P., Xie, C., Ma, Y., He, X., Zhang, Z., Ding, Y., et al. (2017). Shape-dependent transformation and translocation of ceria nanoparticles in cucumber plants. *Environmental Science & Technology Letters, 4*, 380–385.
23. Zook, J. M., MacCuspie, R. I., Locascio, L. E., Halter, M. D., & Elliott, J. T. (2011). Stable nanoparticle aggregates/agglomerates of different sizes and the effect of their size on hemolytic cytotoxicity. *Nanotoxicology, 5*, 517–530.
24. Lin, W., Huang, Y.-w., Zhou, X.-D., & Ma, Y. (2006). Toxicity of cerium oxide nanoparticles in human lung cancer cells. *International Journal of Toxicology, 25*, 451–457.
25. Pešić, M., Podolski-Renić, A., Stojković, S., Matović, B., Zmejkoski, D., Kojić, V., et al. (2015). Anti-cancer effects of cerium oxide nanoparticles and its intracellular redox activity. *Chemico-Biological Interactions, 232*, 85–93.
26. Rubio, L., Annangi, B., Vila, L., Hernández, A., & Marcos, R. (2016). Antioxidant and anti-genotoxic properties of cerium oxide nanoparticles in a pulmonary-like cell system. *Archives of Toxicology, 90*, 269–278.
27. Park, E.-J., Choi, J., Park, Y.-K., & Park, K. (2008). Oxidative stress induced by cerium oxide nanoparticles in cultured BEAS-2B cells. *Toxicology, 245*, 90–100.
28. García-Alonso, J., Rodriguez-Sanchez, N., Misra, S. K., Valsami-Jones, E., Croteau, M. N., Luoma, S. N., et al. (2014). Toxicity and accumulation of silver nanoparticles during development of the marine polychaete Platynereis dumerilii. *The Science of the Total Environment, 476-477*, 688–695.
29. Auffan, M., Rose, J., Wiesner, M. R., & Bottero, J.-Y. (2009). Chemical stability of metallic nanoparticles: A parameter controlling their potential cellular toxicity in vitro. *Environmental Pollution, 157*, 1127–1133.
30. Fröhlich, E. (2012). The role of surface charge in cellular uptake and cytotoxicity of medical nanoparticles. *International Journal of Nanomedicine, 7*, 5577–5591.
31. Yokel, R. A., Unrine, J. M., Wu, P., Wang, B., & Grulke, E. A. (2014). Nanoceria biodistribution and retention in the rat after its intravenous administration are not greatly influenced by dosing schedule, dose, or particle shape. *Environmental Science. Nano, 1*, 549–560.
32. Kamalieva, R., Ishmukhametov, I., Batasheva, S., Rozhina, E., & Fakhrullin, R. (2018). Uptake of halloysite clay nanotubes by human cells: colourimetric viability tests and microscopy study. *Nano-Structures & Nano-Objects, 15*, 54–60.
33. Aljamali, N. M. (2015). Zetasizer technique in biochemistry. *Biochemistry & Analytical Biochemistry, 4*, 1–5.
34. Colon, J., Herrera, L., Smith, J., Patil, S., Komanski, C., Kupelian, P., et al. (2009). Protection from radiation-induced pneumonitis using cerium oxide nanoparticles. *Nanomedicine, 5*, 225–231.